Photonics Review
Photo. Rev. 2025, 250207
https://doi.org/10.11470/photo.250207

Tutorial Review

Topological edge state of light

Tomohiro Amemiya[1*], Sho Okada[1], Hibiki Kagami[1†], Nobuhiko Nishiyama[1], and Xiao Hu[2]

[1]*Department of Electrical and Electronic Engineering, Tokyo Institute of Technology, Tokyo 152-8552, Japan*
[2]*WPI-MANA, National Institute for Materials Science, Ibaraki 305-0044, Japan*
[*]E-mail: amemiya.t.ab@m.titech.ac.jp
[†]Current address: NTT Device Technology Laboratories, Kanagawa-ken 243-0198, Japan

Topological photonics brings the concept of mathematical topology into the field of optics, which allows us to systematically handle information derived from the topology of light, such as optical spin and orbital angular momentum. In this paper, we focus on topological edge states, the most important phenomenon in the field of topological photonics, and describe the specific behavior of an optical spin caused by the states.

Keyword: topological photonics, topological edge states, integrated optics

Received June 13, 2023; Accepted June 14, 2023
Translated from Photonics News **9**, 36 (2023)

Introduction

In recent years, topological phenomena in condensed matter have garnered significant attention, driven by discoveries of novel effects arising from topologically protected surface states and the growing interest in their application to photonic device technologies.[1-4] Motivated by these advances, "topological photonics," has been studied extensively, which applies the concept of topology from electronic systems to photonic systems.[5,6] A distinctive feature of topological photonic systems is their capacity to realize structures with different topological properties by simultaneously controlling intra- and inter-cell interactions within photonic nanoperiodic structures. This dual control enables more flexible photonic band engineering compared to conventional photonic crystals that primarily exploit inter-cell interactions[7-10] and metamaterials that focus mainly on intra-cell interactions.[11-17]

One of the most well-known phenomena in topological photonic systems is the emergence of topological edge states at the interface between two photonic structures with different topologies. These edge states support the propagation of light with specific spin and orbital angular momenta.[18-21] The spin and orbital angular momenta of light corresponding to circular polarization and optical vortices comprise mutually orthogonal sets of modes (with circular polarization supporting two orthogonal states and optical vortices offering a number of orthogonal modes corresponding to the winding number), allowing distinct information to be encoded on each mode.[22] Accordingly, circular polarization and optical vortices are crucial for increasing the capacity of optical transmission. The ability to support and preserve these degrees of freedom within integrated optical circuits highlights the broad potential of topological photonic technologies for a range of practical applications.

Topological Edge States of Light

Topology, or topological geometry, is a branch of mathematics that studies deformable shapes. From this perspective, as illustrated in Fig. 1a, a sphere and a torus may be considered topologically equivalent, since they can be continuously deformed into each other. In this context, the defining characteristic that distinguishes a sphere from a torus is the "number of holes"; objects with different numbers of holes are considered distinct (that is, they have different topologies).

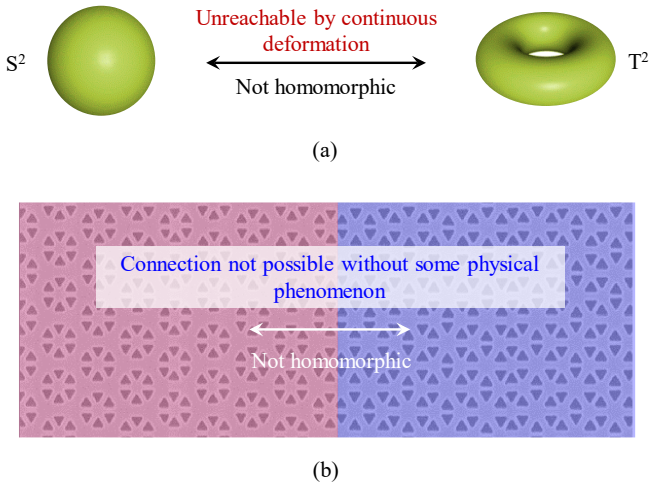

Figure 1 (a) Concept of isomorphism in topological geometry; (b) Concept of isomorphism in photonic structures.

Topological photonics introduces the above concept to the field of optics. However, the idea may be overly abstract, and therefore, we illustrate the idea here using a simple example. Figure 1b shows two photonic structures that possess highly similar optical properties, due to which it may be expected that placing them adjacently would not result in any significant change in optical behavior. However, this is not necessarily the case when the two structures have different topologies. Just as a sphere cannot be continuously deformed into a torus in topological geometry, photonic structures with different topologies cannot be continuously transformed into one another without passing through a special physical state, which is called the "topological edge state" arising at the interface between the two structures. Light propagating through a topological edge state exhibits characteristic behavior with respect to its spin and orbital angular momentum—specifically, circular polarization and optical vortices—as described below.

(1) Property with respect to optical spin: light propagating through a topological edge state exhibits a unique propagation direction determined by the orientation of its circular polarization. Figure 2a shows the H_y component

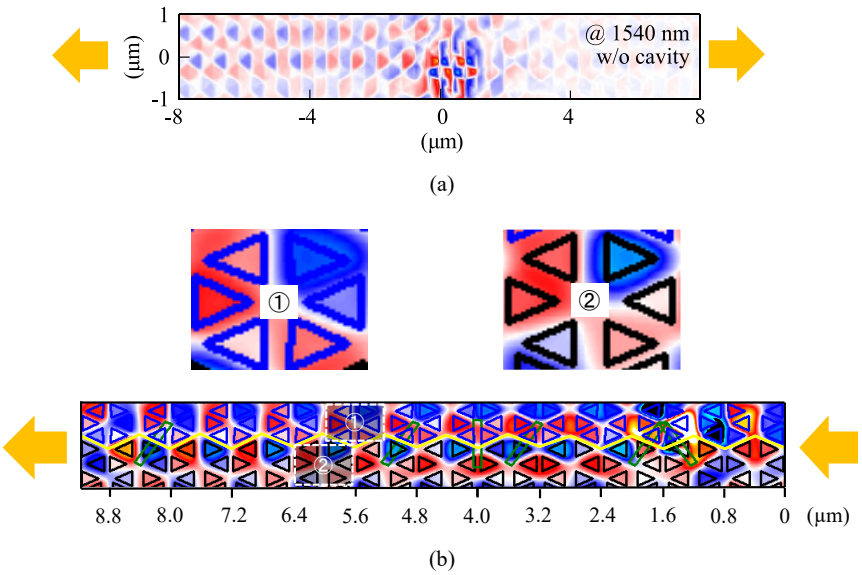

Figure 2 Properties of light propagated by topological edge states: (a) Optical spin (circular polarization); (b) Optical orbital angular momentum (optical vortex).

of light propagating along the adjacent interface when a right circularly polarized plane wave is incident from the top onto the center of the structure shown in Fig. 1b. It can be seen that the light propagates only to the left (if the incident light is left-handed circularly polarized, it propagates along the opposite direction).

(2) Property with respect to optical orbital angular momentum: light propagating through a topological edge state forms localized vortices. Figure 2b shows the H_y component of light propagating along the adjacent interface shown in Fig. 1b. While the energy flow is unidirectional over the entire structure, careful observation shows that the light exhibits localized swirling behavior.

Observing Topology

In light of the above discussion, one question remains: how can we determine whether two photonic structures indeed have different topologies?

In photonic structures, subwavelength-scale features are arranged with a defined periodicity, enabling diverse manipulations of light through light–matter interactions within the structure. One of the key indicators that determine the optical properties of such systems is the photonic band, which represents the dispersion relations of electromagnetic modes within the structure and plays a crucial role in identifying whether two structures are topologically distinct. For instance, in photonic structures with $\mathbb{Z}2$ topology (characterized by two distinct topological phases), the behavior of electromagnetic modes near the bandgap edge, particularly around the Γ-point, can be analyzed to infer the topological nature of the system.

We focus on an experimental demonstration to examine a practical manifestation of this process. Figure 3 shows a scanning electron microscopy (SEM) image of the device used for evaluation. In this experiment, a photonic structure exhibiting $\mathbb{Z}2$ topology was implemented on a silicon-on-insulator (SOI) substrate with a Si layer thickness of 220 nm. The structure comprises triangular nanoholes arranged in a honeycomb lattice with C_{6v} symmetry. The lattice period of the honeycomb structure was fixed at 800 nm, while the

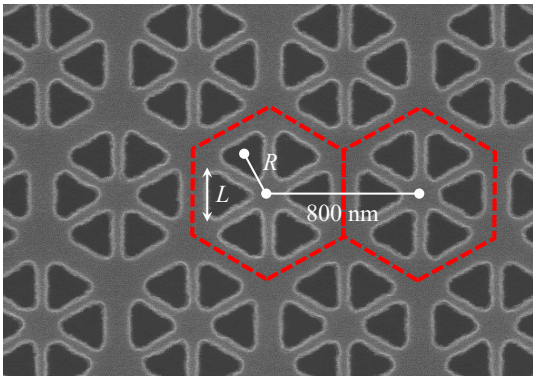

Figure 3 Scanning electron microscope image of a photonic structure exhibiting $\mathbb{Z}2$ topology.

topology of the photonic structure was controlled by varying the distance R from the center of the honeycomb unit to the center of each nanohole and the side length L of the nanoholes. To fabricate the device, ZEP520A was spin-coated onto the SOI substrate, and device patterns were defined using electron beam lithography with proximity effect correction. Subsequently, using ZEP520A as an etching mask, the Si layer was etched by inductively coupled plasma reactive ion etching with an SF_6–C_4F_8 mixed gas.

To rapidly measure the photonic band structure of the fabricated device over a wide angular range, we employed a photonic band microscope based on hyperspectral Fourier imaging spectroscopy.[23] A broadband white light source (Bentham Ltd. WLS100, wavelength range: 300–2500 nm) was used to illuminate the sample perpendicularly through a ×60 objective lens (NA 0.9, Olympus Plan Fluorite Objective, UPLFLN60X). The Fourier image of the light scattered from the device was then observed using a 4f optical system and an infrared camera. A tunable bandpass filter (CRI, VariSpec LNIR, bandwidth: 6 nm) was placed in front of the infrared camera, enabling the acquisition of diffraction patterns at arbitrary wavelengths within the 850–1800 nm range.

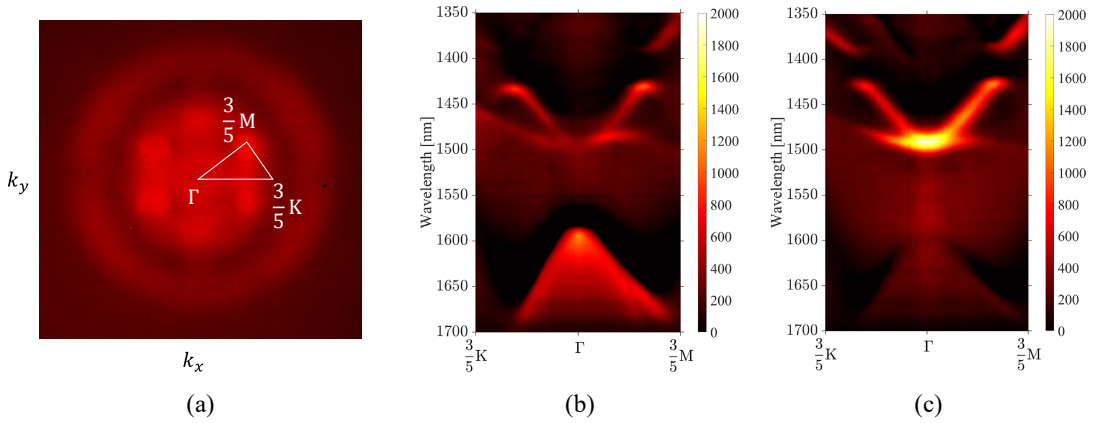

Figure 4 (a) Fourier images of scattered light from the photonic structure; (b), (c) Band measurement results for two representative photonic structures with different topologies.

Using this configuration, the procedure for obtaining the photonic band diagram is as follows. The entire process was fully automated via software to ensure both high-speed operation and versatility. First, while varying the center wavelength of the tunable filter, Fourier images of the light scattered from the device were acquired. Next, intensity information along a specified path was extracted from each Fourier image and converted into the intensity distribution at a given energy in reciprocal space. Finally, by repeating the above operations for all wavelengths, the photonic band structure was obtained.

Figure 4 presents the measurement results for two representative photonic structures with different topologies, characterized by $(R, L) = (230\,\text{nm}, 250\,\text{nm})$ and $(290\,\text{nm}, 250\,\text{nm})$, respectively. Figure 4a shows the Fourier images of light scattered from the devices, in which pronounced wavelength-dependent changes attributed to the photonic bands are clearly observed. By measuring the intensity along the Γ-K-M path corresponding to the honeycomb lattice in Fig. 4a, the reconstructed photonic bands are shown in Figs. 4b and 4c. In both cases, a photonic bandgap was observed near the optical communication band at approximately 1.5 μm. Notably, the intensity distribution at the upper and lower band edges near the Γ-point is reversed between the two structures. These experimental results suggest that the electromagnetic modes associated with the pp- and dd-like bands are inverted at the Γ-point (the reflectivity of the dd-like mode is generally weaker than that of the pp-like mode), thereby allowing us to observe the distinct topologies between the two structures.[24)]

Optical Spin Transport in Topological Edge States

As described earlier, light propagating through topological edge states exhibits distinctive properties with respect to its spin and orbital angular momenta. In this section, we focus on the spin component (circular polarization) and examine how light exhibits unique behavior when propagating along the interface formed by placing two photonic structures with different topologies in contact.

Figure 5 shows an SEM image of the device used in this study. Two photonic structures with different topologies are joined via a zigzag-type interface, where edge states emerge to form a topological waveguide. To enhance the vertical coupling efficiency of the device, triangular nanoholes were removed from specific lattice sites near the topological

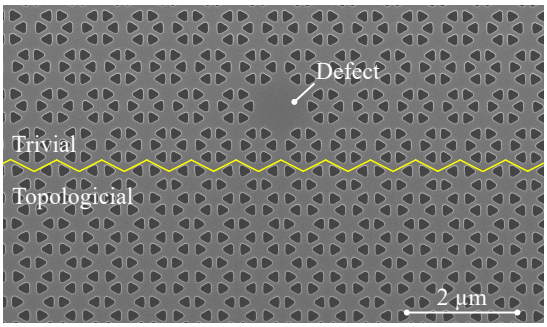

Figure 5 Scanning electron microscope image of the device used to observe the properties of topological edge states.

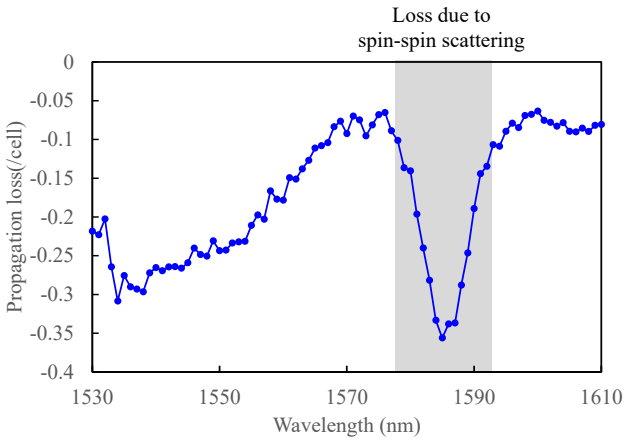

Figure 6 Wavelength dependence of the propagation characteristics of a topological waveguide without defect structures.

waveguide; these regions are hereafter referred to as "defect structures."[25-27)] In the defect structures, the honeycomb lattice is filled with a high-refractive-index dielectric, forming a cavity that strongly confines vertically incident light. At the same time, the surrounding topological edge states are disrupted, allowing the confined light to couple efficiently into the topological waveguide.

Figure 6 shows the wavelength dependence of the propagation characteristics of the topological waveguide without defect structures. Low-loss propagation (~0.1 dB/cell) is achieved within the photonic bandgap range observed in Figs. 4b and 4c. Additionally, a reduction in propagation loss

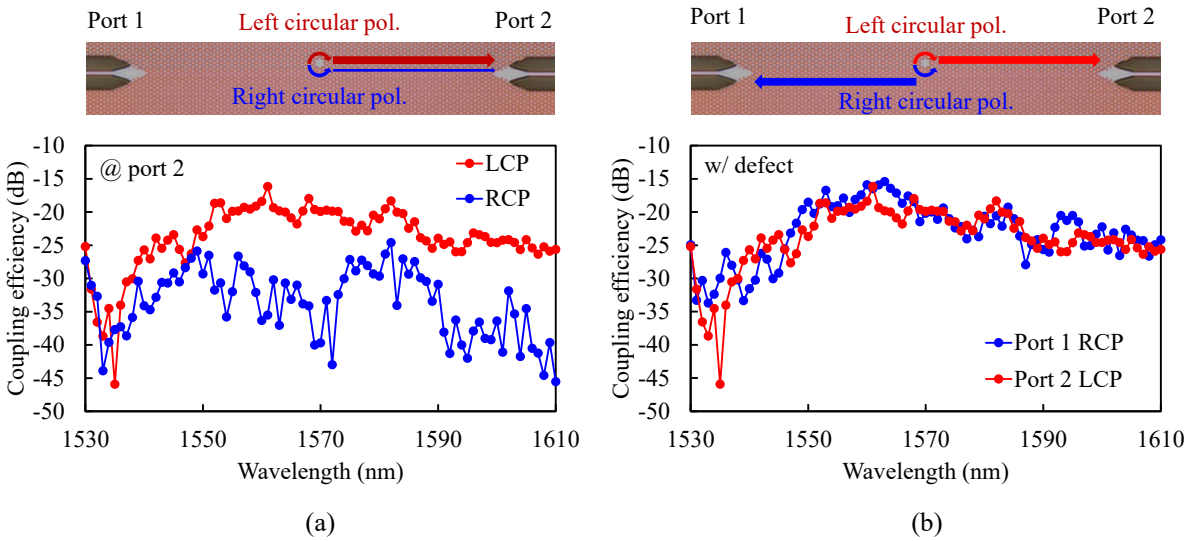

Figure 7 Wavelength dependence of output intensity from each port when left- and right-handed circularly polarized light is incident: (a) Output intensity from the same port for both circular polarizations; (b) Output intensity from different ports corresponding to each circular polarization.

associated with spin–spin scattering is observed near the bandgap center at approximately 1,580–1,590 nm. These results confirm that a topological edge state emerges at the interface between the two photonic structures and that light propagation occurs via this edge state.

Next, the spin properties of light were examined by injecting light vertically into a topological waveguide with defect structures. In this experiment, a tunable-wavelength laser was coupled to a polarization-maintaining optical fiber and collimated through a lens. A linear polarizer and quarter-wave plate were then used to generate left- and right-handed circularly polarized waves. The light was incident onto the device from above via an objective lens (Olympus LCPLFLN20XLCD, NA 0.9). After propagating through the topological waveguide, the output light was collected by a polarization-maintaining fiber and analyzed using a spectrum analyzer and power monitor to evaluate its propagation characteristics. To eliminate stray light, an inline polarizer was inserted into the output-side polarization-maintaining fiber.

Figure 7 shows the wavelength dependence of the output intensity from each port when left- and right-handed circularly polarized light is incident on the device. Figure 7a presents the output intensity from a single port for both polarizations, revealing a characteristic feature of the topological edge state in which a specific circular polarization propagates unidirectionally: when the incident light is right-handed circularly polarized, the output is dominant at port 1; when left-handed, it is dominant at port 2. In the operating wavelength range of the defect structure (1,550–1,580 nm), the intensity ratio between the two ports reached approximately 20 dB at maximum. Figure 7b shows the output intensity from the respective dominant ports for each polarization. Nearly identical propagation characteristics were obtained in both directions, clearly reflecting the spin-dependent nature of the topological edge state.

Conclusion

In this article, we have described the topological edge states that arise at the interface between two photonic structures with different topologies. As discussed above, light propagating through such edge states exhibits a unique phenomenon in which the propagation direction is determined unambiguously by the handedness of circular polarization. When left- and right-handed circular polarizations are interpreted as the photonic analogs of spin-up and spin-down states, this behavior can be interpreted as an optical analogue of spin-momentum locking observed in topological insulators.

Topological photonics is an interdisciplinary field at the intersection of mathematics, optics, and solid-state physics, with particular emphasis on studying phenomena from multidisciplinary perspectives. By directly observing the phenomena and engaging in cross-disciplinary discussions, a deeper and more comprehensive understanding of these systems can be achieved.

Acknowledgments

The research presented in this article was supported by JST-CREST (JPMJCR18T4), JST-ASTEP (JPMJTR22RG), and JSPS KAKENHI (Grant No. 22H01520).

References

1) Hasan, M. Z. and Kane, C. L.: "Colloquium: Topological insulators," Rev. Mod. Phys., **82** (2010) 3045-3067.
2) Qi, X.-L. and Zhang, S.-C.: "Topological insulators and superconductors," Rev. Mod. Phys., **83** (2011) 1057-1110.
3) Xiao, D., et al.: "Berry phase effects on electronic properties," Rev. Mod. Phys., **82** (2010) 1959-2007.
4) Weng, H., et al.: "Quantum anomalous Hall effect and related topological electronic states," Adv. Phys., **64** (2015) 227-282.
5) Wang, Z., et al.: "Observation of unidirectional backscattering-immune topological electromagnetic states," Nature, **461** (2009) 772-775.
6) Ozawa, T., et al.: "Topological photonics," Rev. Mod. Phys., **91** (2019) 015006.
7) Joannopoulos, J., et al.: "Photonic crystals: putting a new twist on light," Nature, **386** (1997) 143-149.
8) Baba, T.: "Slow light in photonic crystals," Nature photonics, **2** (2008) 465-473.
9) Kondo, K., et al.: "Fan-beam steering device using a photonic crystal slow-light waveguide with surface diffraction grating," Opt. Lett. **42** (2017) 4990-4993.
10) Asano, T., et al.: "Photonic crystal nanocavity with a Q factor exceeding eleven million," Opt. Express, **25** (2017) 1769-1777.
11) Pendry, J. B., et al.: "Magnetism from conductors and enhanced nonlinear phenomena," IEEE Trans. Microw. Theory Techn., **47** (1999) 2075-2084.

12) Shelby, R. A., et al.: "Experimental verification of a negative index of refraction," Science, **292** (2001) 77-79.
13) Amemiya, T., et al.: "Nonunity permeability in metamaterial-based GaInAsP/InP multimode interferometers," Opt. Lett., **36** (2011) 2327-2329.
14) Zheldev N. I. and Kivshar, Y. S.: "From metamaterials to metadevices," Nature Materials, **11** (2012) 917-924.
15) Amemiya, T., et al.: "Metamaterial waveguide devices for integrated optics," Materials, **10** (2017) 1037.
16) Amemiya, T., et al.: "Demonstration of slow-light effect in silicon-wire waveguides combined with metamaterials," Opt. Express, **27** (2019) 15007-15017.
17) Tanaka, M., et al.: "Control of slow-light effect in a metamaterial-loaded Si waveguide," Opt. Express, **28** (2020) 23198-23208.
18) Wu, L.-H., et al.: "Scheme for achieving a topological photonic crystal by using dielectric material," Phys. Rev. Lett., **114** (2015) 223901.
19) Kim, M., et al.: "Spin-valley locked topological edge states in a staggered chiral photonic crystal," New J. Phys., **22** (2020) 113022.
20) Parapppurath, N., et al.: "Direct observation of topological edge states in silicon photonic crystals: Spin, dispersion, and chiral routing," Sci. Adv., **6** (2020) eaaw4137.
21) Wang, X.-X., et al.: "Interference and switching effect of topological interfacial modes with geometric phase," Phys. Rev. Res., **7** (2025) 023067.
22) Liu, J., et al.: "1-Pbps orbital angular momentum fibre-optic transmission," Light Sci. Appl., **11** (2022) 202.
23) Amemiya, T., et al.: "High-speed infrared photonic band microscope using hyperspectral Fourier image spectroscopy," Opt. Lett., **47** (2022) 2430-2433.
24) Okada, S., et al.: "Discussion on fabrication accuracy of infrared topological photonic structures using hyperspectral Fourier image spectroscopy," J. Opt. Soc. Am. B, **39** (2022) 2464-2469.
25) Kagami, H., et al.: "Highly efficient vertical coupling to a topological waveguide with defect structure," Opt. Express, **29** (2021) 32755-32763.
26) Kagami, H., et al.: "Selective excitation of optical vortex modes with specific charge numbers in band-tuned topological waveguides," Opt. Lett., **47** (2022) 2190-2193.
27) Okada, S., et al.: "Demonstration of a highly efficient topological vertical coupler," Opt. Express, **31** (2023) 35218-35224.